Supplement of Atmos. Chem. Phys., 16, 9891–9903, 2016
http://www.atmos-chem-phys.net/16/9891/2016/
doi:10.5194/acp-16-9891-2016-supplement

Atmospheric Chemistry and Physics
Open Access

Supplement of

Oxidative capacity and radical chemistry in the polluted atmosphere of Hong Kong and Pearl River Delta region: analysis of a severe photochemical smog episode

Likun Xue et al.

Correspondence to: Likun Xue (xuelikun@sdu.edu.cn)

Table S1. Summary of field measurements at Tung Chung in summer 2011

Species	**Instrument or techniques**	**Time resolution**
O_3	*TEI 49i*	1 min
CO	*API 300EU*	1 min
SO_2	*TEI 43i*	1 min
NO & NO_2	*TEI 42i + blue light converter*	1 min
NO & NOy	*TEI 42cy + MoO converter*	1 min
HONO	*LOPAP*	1 min
$ClNO_2$	*CIMS*	6 sec
PANs	*CIMS*	6 sec
H_2O_2 & organic peroxides	*Aerolaser AL-2021*	1 min
C_1-C_{10} hydrocarbons	*Canister + GC/FID/ECD/MS*	24-hour
C_2-C_{10} hydrocarbons	*Syntech Spectras, model GC955 Series 600/800 POCP*	30 min
C_1-C_8 carbonyls	*DNPH-coated sorbent cartridge sampling + HPLC*	24-hour in general; 3-hour on episode
$PM_{2.5}$ & PM_{10} mass	*SHARP*	1 min
SO_4^{2-}, NO_3^-, NH_4^+, Cl^-, Na^+, Ca^{2+}, K^+ in $PM_{2.5}$	*MARGA*	1 hour
OC & EC in $PM_{2.5}$	*Sunset OCEC analyzer*	1 hour
BC in $PM_{2.5}$	*Magee*	5 min
Aerosol scattering coefficient	*Ecotech Nephelometer*	1 min
Particle number concentration (5 nm-10 μm)	*MSP/WPS Model 1000XP*	8 min
J_{NO2}	*Metcon Filter Radiometer*	5 sec
Temperature & RH	*Young RH/T probe*	5 sec
Wind speed and direction	*Gill WindSonic*	5 sec
Solar Radiation	*LI-200 Pyranometer Sensor*	5 sec

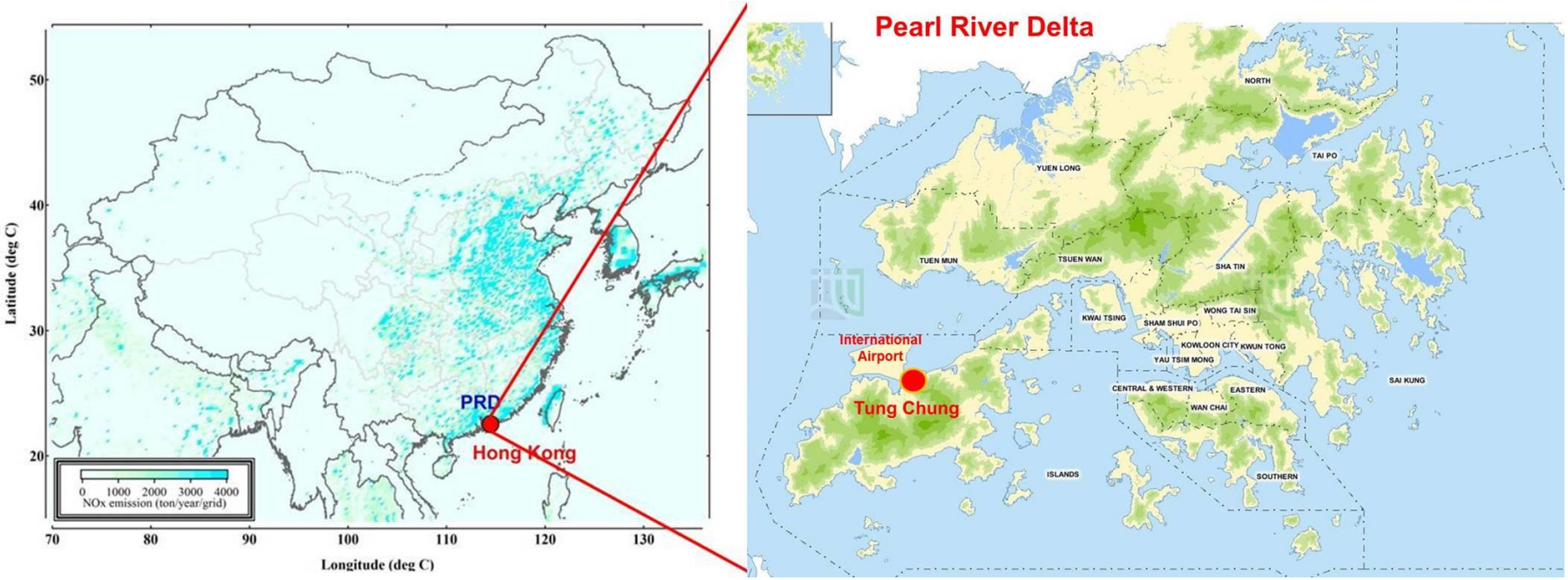

Figure S1. Map showing the locations of Hong Kong, the Pearl River Delta region and the study site at Tung Chung (TC).

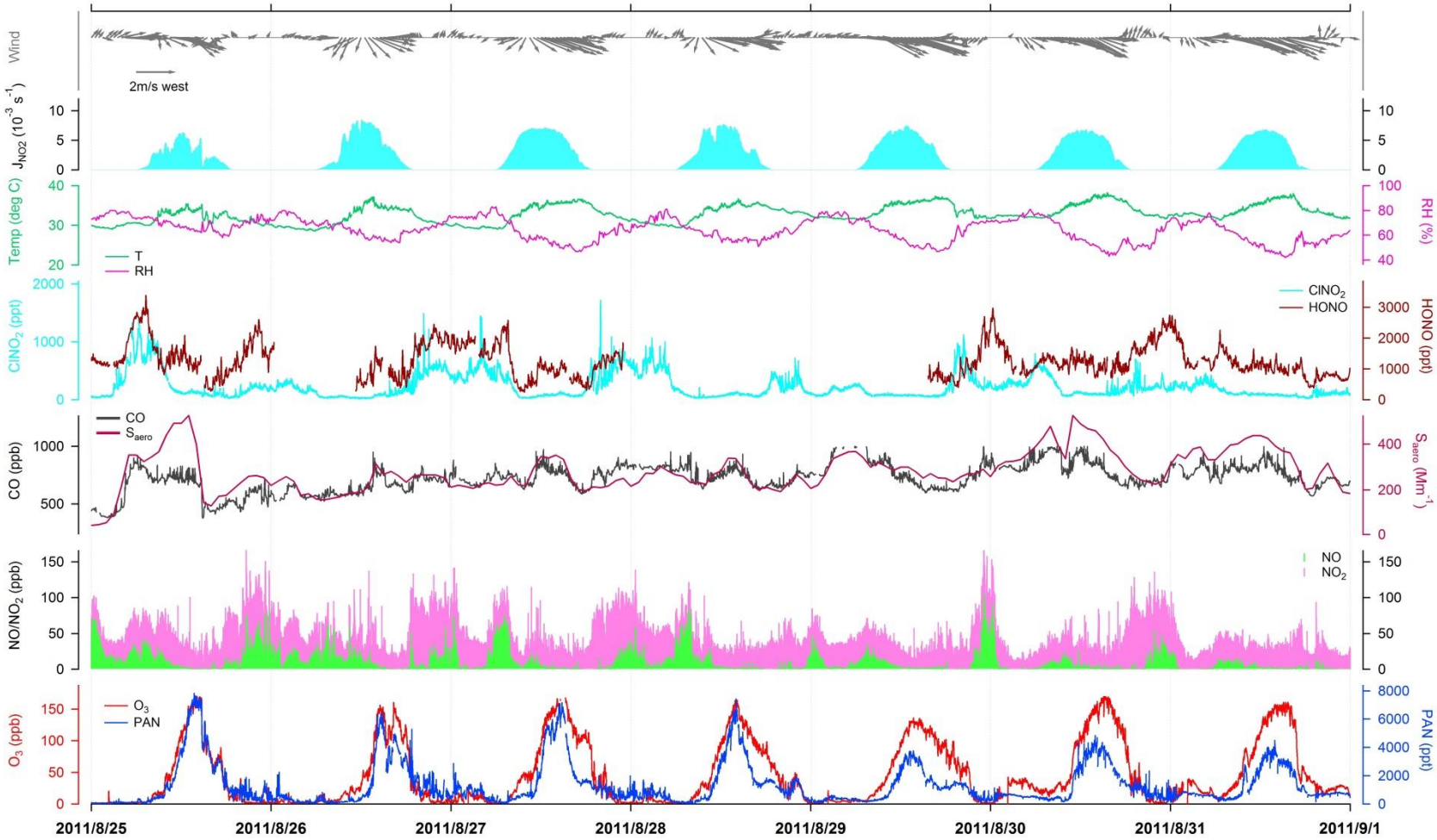

Figure S2. Time series of air pollutants and meteorological parameters observed at Tung Chung from 25-31 August 2011. S_{aero} stands for the scattering coefficient of $PM_{2.5}$. The data gap for HONO was mainly due to the calibration and maintenance of the instrument.

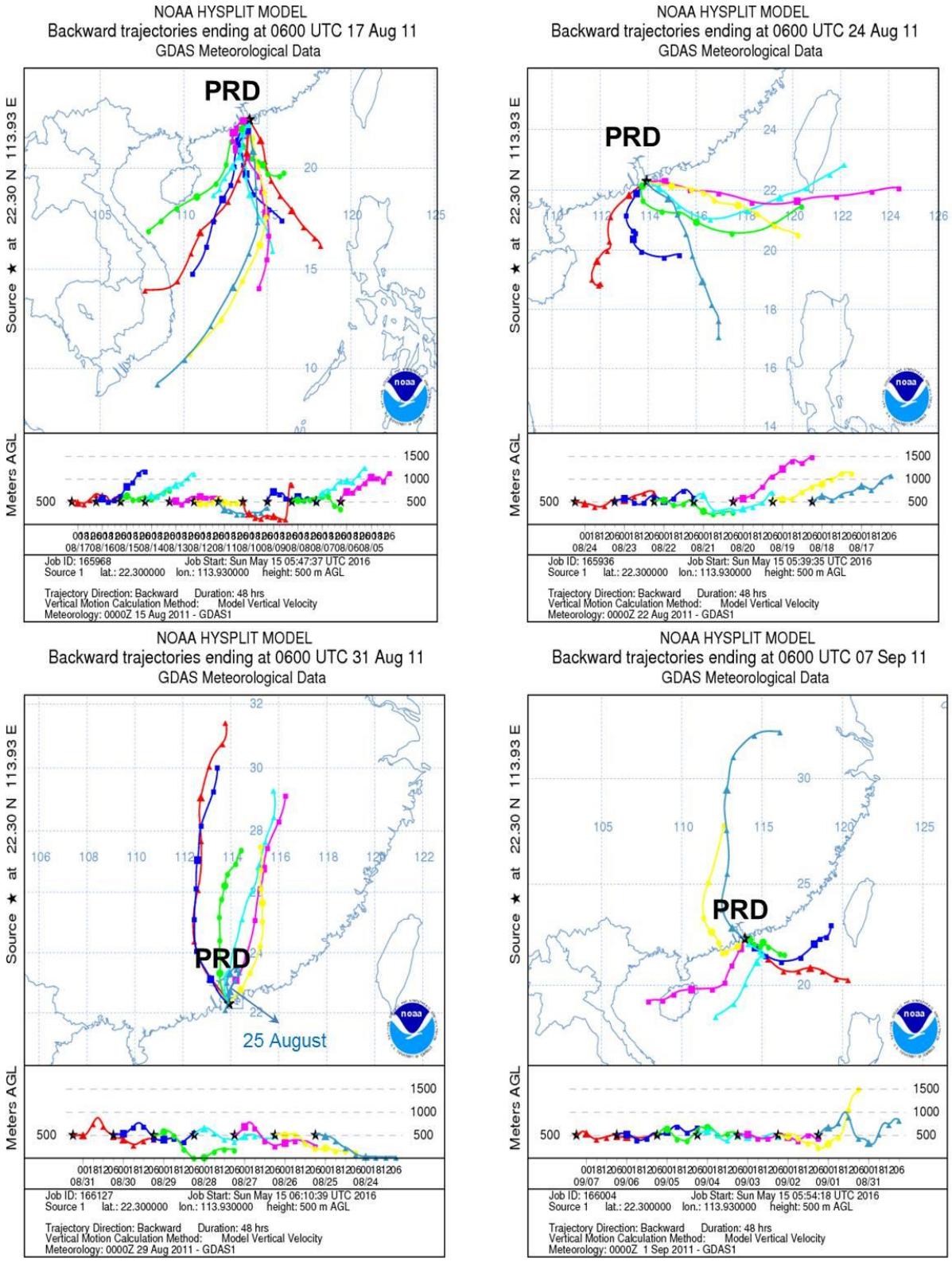

Figure S3. 48-hour backward trajectories calculated by the HYSPLIT model for air masses at TC at 12:00 LT each day from 6th August to 7th September. The height of the starting point was set as 500 m a.g.l. See the lower panels for the legend of trajectories each day.

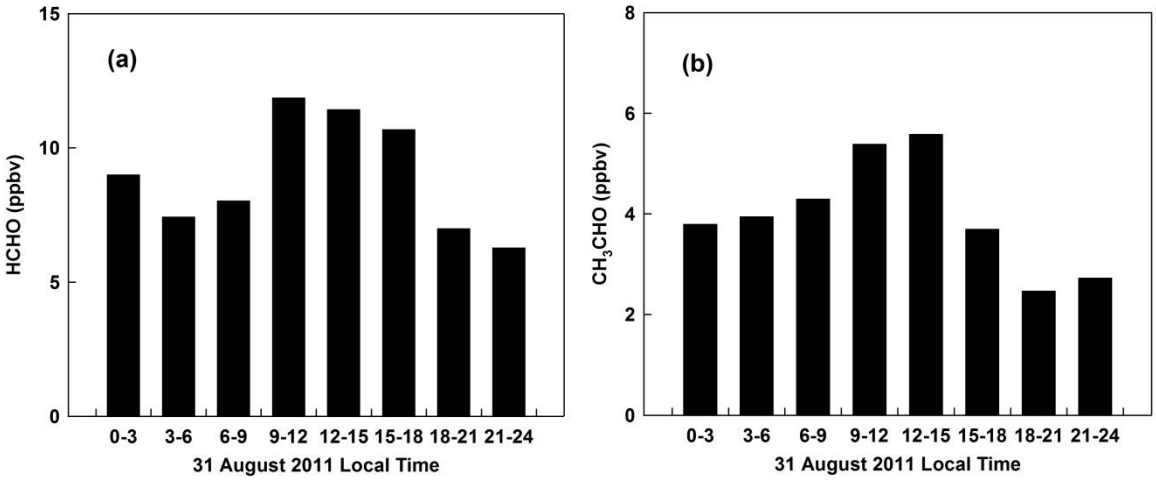

Figure S4. Diurnal variations of (a) formaldehyde and (b) acetaldehyde measured at Tung Chung on 31 August 2011.

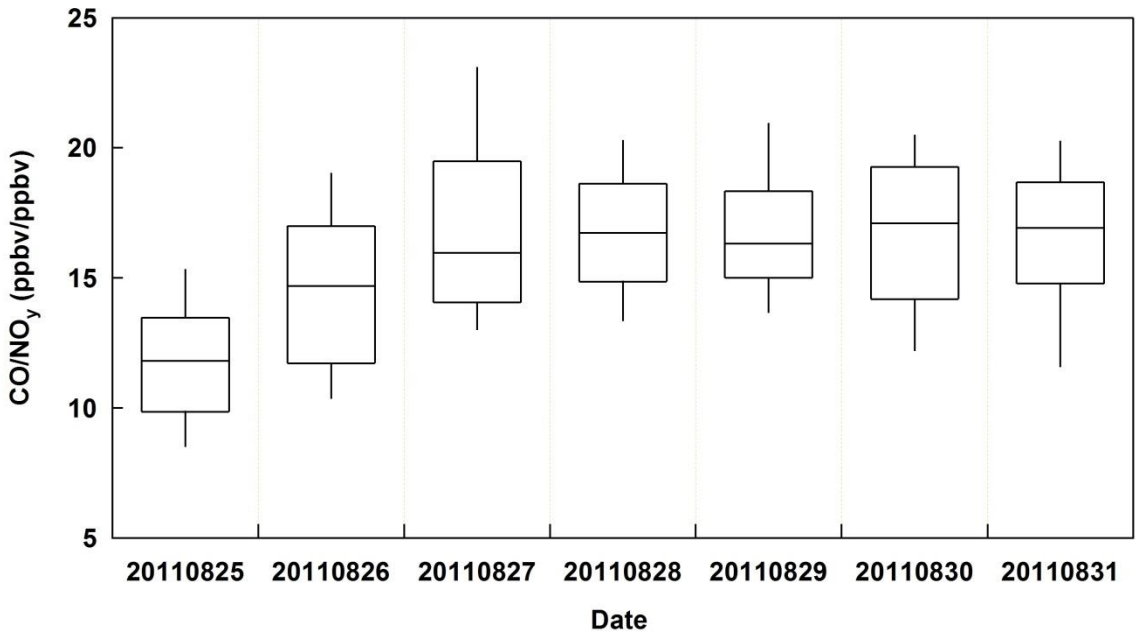

Figure S5. Distributions of the daytime (08:00–18:00 local time) CO/NO_y ratios measured at Tung Chung from 25–31 August 2011. The whisker plot provides the 90th, 75th, 50th, 25th and 10th percentiles of the measurement data.

1. Details of the OBM-AOCP model

The OBM-AOCP (Observation-Based Model for investigating the Atmospheric Oxidative Capacity and Photochemistry) is a zero-dimensional chemical box model that is capable of predicting the concentrations of reactive species (e.g., radicals) and quantifying the rates of various atmospheric photochemical processes. It has been used for evaluation of O_3 and PAN formation, radical budget, and heterogeneous photochemistry in many previous studies (e.g., Xue et al., 2013; 2014a; 2014b; 2014c; 2015). The configuration of this model is detailed as follows.

1.1. Chemical mechanisms

1.1.1. Basic mechanism

The OBM-AOCP is built on the Master Chemical Mechanism (MCM, *v3.2*). MCM is a nearly explicit mechanism describing the gas phase degradation of 143 primarily emitted VOC species together with the latest inorganic chemistry. It involves about 6700 chemical species (including intermediates and products) and includes approximately 17000 reactions. The detailed description of the MCM has been provided by Jenkin et al. (2003) and Saunders et al. (2003).

1.1.2. Heterogeneous chemistry module

In addition, the OBM-AOCP also incorporated a chemistry module describing several key heterogeneous processes in the atmosphere, namely, heterogeneous loss of N_2O_5 on particle surface and subsequent formation of $ClNO_2$, reactions of NO_2 on aerosol and ground surfaces producing HONO, uptake of HO_2 and NO_3 on aerosol surfaces, and heterogeneous reactions of HOCl and $ClONO_2$ on aerosol surface. The chemical reactions and related parameters, which are relevant to the present study, have been summarized in *Table S2*.

Table S2. Summary of the heterogeneous reactions incorporated into the OBM-AOCP

Heterogeneous Reaction	k (cm^3 molecules^{-1} s^{-1})	Remarks
$N_2O_5 \rightarrow NA + ClNO_2$	$0.25\times v_{N2O5}\times \gamma_{N2O5}\times S_{AERO}\times \varphi_{ClNO2}$	a
$N_2O_5 \rightarrow NA + NA$	$0.25\times v_{N2O5}\times \gamma_{N2O5}\times S_{AERO}\times (1-\varphi_{ClNO2})$	a
$HO_2 \rightarrow$ products	$-(\frac{r}{Dg}+\frac{4}{\gamma HO2}\times v_{HO2})^{-1}\times S_{AERO}$	b

$NO_3 \rightarrow$ products	$0.25\times v_{NO3}\times\gamma_{NO3}\times S_{AERO}$	c
$ClONO_2 \rightarrow Cl_2 + HNO_3$	$0.25\times v_{ClONO2}\times\gamma_{ClONO2}\times S_{AERO}$	d
$HOCl \rightarrow Cl_2$	$0.25\times v_{HOCl}\times\gamma_{HOCl}\times S_{AERO}$	e
$NO_2 \rightarrow HONO$	aerosol: $\frac{1}{4}\times v_{NO2}\times\gamma_{NO2\_a}\times S_{AERO}$	f
	ground: $\frac{1}{8}\times v_{NO2}\times\gamma_{NO2\_g}\times\frac{S}{V}$	f

v_x: mean molecular speed of x; γ_x: uptake coefficient of x on surfaces; S_{AERO}: aerosol surface area concentration.

[a] φ_{ClNO2}: product yield of $ClNO_2$ from heterogeneous reaction of N_2O_5. In the present study, we turned off the formation of $ClNO_2$ and constrained the model with the measured $ClNO_2$ profiles. We adopted a moderate γ_{N2O5} of 0.014 in the present study, which was the observationally-derived average value from our recent field study in Hong Kong (Wang et al., 2016). NA: nitrate aerosol.

[b] *r*: surface-weighted particle radius; *D*g: gas phase diffusion coefficient. In the present study, we adopted a moderate γ_{HO2} value of 0.02.

[c] γ_{NO3} =0.004.

[d] γ_{ClONO2} =0.01.

[e] γ_{HOCl} =0.01.

[f] $\gamma_{NO2\_g/a}$: uptake coefficient of NO_2 on ground/aerosol surfaces. Considering the photo-enhanced production of HONO from surface reactions, higher values of $\gamma_{NO2\_g/a}$ were used during daytime than at night. For γ_{NO2_a}, we used a value of 1×10^{-6} at nighttime and increased it to 5×10^{-6} during daytime. For γ_{NO2_g}, when solar radiation was smaller than 400 W m^{-2}, we used the values of 1×10^{-6} and 2×10^{-5} during night and daytime respectively; with more intense solar radiation, γ_{NO2_g} = $2\times10^{-5}\times$(solar radiation/400) was used. *S/V* refers to the effective surface density of the ground. An effective surface area of 1.7 m^2 per geometric ground surface was used to calculate the *S/V*. Please refer to *Xue et al.* (2014a) for the details.

1.1.3. Chlorine chemistry module

The MCM (*v3.2*) only considers the reactions of chlorine atom (Cl·) with alkane species (Saunders et al., 2003). To comprehensively represent the Cl· chemistry, we have developed a detailed chlorine chemistry module and incorporated it into the OBM-AOCP. The protocol for compiling this new chemistry scheme has been published in recent (Xue et al., 2015), and the code in the format of FACSIMILE language is freely available per request. The chemical reactions and kinetic data are summarized below in *Tables S3-S5*.

Table S3. Summary of inorganic reactions added in the MCM to represent chlorine chemistry

Category	Reactions	*k* (cm^3 $molecules^{-1}$ s^{-1}) or *J* (s^{-1})	Remarks

Photolysis reactions	$Cl_2 \rightarrow Cl + Cl$	J_{Cl2}	-
	$ClNO_2 \rightarrow NO_2 + Cl$	J_{ClNO2}	a
	$ClONO_2 \rightarrow NO_3 + Cl$	$0.83\times J_{ClONO2}$	b
	$ClONO_2 \rightarrow NO_2 + ClO$	$0.17\times J_{ClONO2}$	b
	$HOCl \rightarrow OH + Cl$	J_{HOCl}	-
Cl + X	$Cl + O_3 \rightarrow ClO + O_2$	$2.8\times10^{-11}\times\exp(-250/T)$	c
	$Cl + HO_2 \rightarrow HCl + O_2$	3.5×10^{-11}	c
	$Cl + HO_2 \rightarrow ClO + OH$	$7.5\times10^{-11}\times\exp(-620/T)$	c
	$Cl + H_2O_2 \rightarrow HCl + HO_2$	$1.1\times10^{-11}\times\exp(-980/T)$	c
	$Cl + NO_3 \rightarrow NO_2 + ClO$	2.4×10^{-11}	c
	$Cl + ClONO_2 \rightarrow Cl_2 + NO_3$	$6.2\times10^{-12}\times\exp(145/T)$	c
OH + *X*	$OH + HCl \rightarrow Cl + H_2O$	$1.7\times10^{-12}\times\exp(-230/T)$	c
	$OH + Cl_2 \rightarrow HOCl + Cl$	$3.6\times10^{-12}\times\exp(-1200/T)$	c
	$OH + HOCl \rightarrow ClO + H_2O$	5.0×10^{-13}	c
	$OH + ClO \rightarrow HO2 + Cl$	1.8×10^{-11}	c
	$OH + ClO \rightarrow HCl + O_2$	1.2×10^{-12}	c
ClO + *X*	$ClO + NO_2 \rightarrow ClONO_2$	7.0×10^{-11}	c
	$ClO + HO_2 \rightarrow HOCl + O_2$	$2.2\times10^{-12}\times\exp(340/T)$	c
	$ClO + NO \rightarrow Cl + NO_2$	$6.2\times10^{-12}\times\exp(295/T)$	c
Heterogeneous reactions	$N_2O_5 \rightarrow NA + NA$	$0.25\times v_{N2O5}\times\gamma_{N2O5}\times S_{AERO}\times(1-\varphi_{ClNO2})$	d
	$N_2O_5 \rightarrow NA + ClNO_2$	$0.25\times v_{N2O5}\times\gamma_{N2O5}\times S_{AERO}\times\varphi_{ClNO2}$	d
	$ClONO_2 \rightarrow Cl_2 + HNO_3$	$0.25\times v_{ClONO2}\times\gamma_{ClONO2}\times S_{AERO}$	d
	$HOCl \rightarrow Cl_2$	$0.25\times v_{HOCl}\times\gamma_{HOCl}\times S_{AERO}$	d

[a] In the present study, J_{ClNO2} was scaled as a function of the measured J_{NO2}, i.e., $J_{ClNO2} = 0.040*J_{NO2}$.

[b] The branching ratio is determined based on the Tropospheric Ultraviolet Visible (TUV) Radiation model calculations (http://cprm.acd.ucar.edu/Models/TUV/Interactive_TUV/).

[c] The kinetic data are taken from the IUPAC database (http://iupac.pole-ether.fr/index.html).

[d] The same as those described in Table S2.

Table S4. Summary of organic reactions existing in the MCM to represent chlorine chemistry

Reactions	***k* (cm^3 molecules^{-1} s^{-1})**
Cl + CH4 = CH3O2 + HCl	$6.6\times10^{-12}\times\exp(-1240/T)$
Cl + C2H6 = C2H5O2 + HCl	$8.3\times10^{-11}\times\exp(-100/T)$
Cl + C3H8 = IC3H7O2 + HCl	$0.43\times1.4\times10^{-10}\times\exp(75/T)$
Cl + C3H8 = NC3H7O2 + HCl	$0.59\times1.4\times10^{-10}\times\exp(-90/T)$
Cl + NC4H10 = NC4H9O2 + HCl	$0.44\times2.05\times10^{-10}\times\exp(-120/T)$
Cl + NC4H10 = SC4H9O2 + HCl	$0.59\times2.05\times10^{-10}\times\exp(55/T)$
Cl + IC4H10 = IC4H9O2 + HCl	$0.564\times1.43\times10^{-10}$

Cl + IC4H10 = TC4H9O2 + HCl	$0.436\times1.43\times10^{-10}$
Cl + NC5H12 = PEAO2 + HCl	$0.222\times2.80\times10^{-10}$
Cl + NC5H12 = PEBO2 + HCl	$0.558\times2.80\times10^{-10}$
Cl + NC5H12 = PECO2 + HCl	$0.220\times2.80\times10^{-10}$
Cl + IC5H12 = IPEAO2 + HCl	$0.408\times2.20\times10^{-10}$
Cl + IC5H12 = IPEBO2 + HCl	$0.342\times2.20\times10^{-10}$
Cl + IC5H12 = IPECO2 + HCl	$0.250\times2.20\times10^{-10}$
Cl + NEOP = NEOPO2 + HCl	1.11×10^{-10}
Cl + NC6H14 = HEXAO2 + HCl	$0.182\times3.40\times10^{-10}$
Cl + NC6H14 = HEXBO2 + HCl	$0.457\times3.40\times10^{-10}$
Cl + NC6H14 = HEXCO2 + HCl	$0.361\times3.40\times10^{-10}$
Cl + M2PE = M2PEAO2 + HCl	$0.321\times2.90\times10^{-10}$
Cl + M2PE = M2PEBO2 + HCl	$0.269\times2.90\times10^{-10}$
Cl + M2PE = M2PECO2 + HCl	$0.213\times2.90\times10^{-10}$
Cl + M2PE = M2PEDO2 + HCl	$0.197\times2.90\times10^{-10}$
Cl + M3PE = M3PEAO2 + HCl	$0.317\times2.80\times10^{-10}$
Cl + M3PE = M3PEBO2 + HCl	$0.530\times2.80\times10^{-10}$
Cl + M3PE = M3PECO2 + HCl	$0.153\times2.80\times10^{-10}$
Cl + M22C4 = M22C43O2 + HCl	$0.461\times1.71\times10^{-10}$
Cl + M22C4 = M33C4O2 + HCl	$0.386\times1.71\times10^{-10}$
Cl + M22C4 = M22C4O2 + HCl	$0.154\times1.71\times10^{-10}$
Cl + M23C4 = M23C43O2 + HCl	$0.478\times2.30\times10^{-10}$
Cl + M23C4 = M23C4O2 + HCl	$0.522\times2.30\times10^{-10}$
Cl + NC7H16 = HEPTO2 + HCl	3.90×10^{-10}
Cl + M2HEX = M2HEXAO2 + HCl	$0.779\times3.50\times10^{-10}$
Cl + M2HEX = M2HEXBO2 + HCl	$0.221\times3.50\times10^{-10}$
Cl + M3HEX = M3HEXAO2 + HCl	$0.793\times3.11\times10^{-10}$
Cl + M3HEX = M3HEXBO2 + HCl	$0.207\times3.11\times10^{-10}$
Cl + NC8H18 = OCTO2 + HCl	4.60×10^{-10}
Cl + NC9H20 = NONO2 + HCl	4.80×10^{-10}
Cl + NC10H22 = DECO2 + HCl	5.55×10^{-10}
Cl + NC11H24 = UDECO2 + HCl	6.17×10^{-10}
Cl + NC12H26 = DDECO2 + HCl	6.74×10^{-10}
Cl + CHEX = CHEXO2 + HCl	3.50×10^{-10}

Table S5. Summary of organic reactions added to the MCM to represent the chlorine chemistry

Reactions [a]	***k*** ***(cm^{3}molecules^{-1}s^{-1})***	**Source**
	Aldehydes + Cl	
HCHO + Cl → HCl + HO2 + CO	$8.1\times10^{-11}\times\exp(-34/T)$	IUPAC

CH3CHO + Cl → CH3CO3 + HCl	7.92×10^{-11}	IUPAC
CH3CHO + Cl → HCOCH2O2 + HCl	8.0×10^{-13}	IUPAC
C2H5CHO + Cl → C2H5CO3 + HCl	1.3×10^{-10}	IUPAC
C3H7CHO + Cl → BUTALO2 + HCl	$5.5\times10^{-12}\times\exp(410/T)$	b
C3H7CHO + Cl → C3H7CO3 + HCl	$3.1\times10^{-11}\times\exp(410/T)$	b
IPRCHO + Cl → IBUTALBO2 + HCl	$2.2\times10^{-12}\times\exp(410/T)$	b
IPRCHO + Cl → IBUTALCO2 + HCl	$2.4\times10^{-12}\times\exp(410/T)$	b
IPRCHO + Cl → IPRCO3 + HCl	$3.7\times10^{-11}\times\exp(410/T)$	b
C4H9CHO + Cl → C4CHOBO2 + HCl	$7.3\times10^{-12}\times\exp(448/T)$	b
C4H9CHO + Cl → C4H9CO3 + HCl	$3.1\times10^{-11}\times\exp(448/T)$	b
BENZAL + Cl → C6H5CO3 + HCl	$3.6\times10^{-11}\times\exp(225/T)$	b
GLYOX + Cl → CO + CO + HO2 + HCl	$4.86\times10^{-11}\times\exp(-34/T)$	c
GLYOX + Cl → HCOCO3 + HCl	$3.24\times10^{-11}\times\exp(-34/T)$	c
MGLYOX + Cl → CH3CO3 + CO + HCl	8.0×10^{-11}	c
MACR + Cl → MACO3 + HCl	$4.86\times10^{-11}\times\exp(380/T)\times0.45$	d
Ketones + Cl		
CH3COCH3 + Cl → CH3COCH2O2 + HCl	$1.5\times10^{-11}\times\exp(-590/T)$	IUPAC
MEK + Cl → MEKAO2 + HCl	$1.4\times10^{-11}\times\exp(80/T)$	IUPAC
MEK + Cl → MEKBO2 + HCl	$1.4\times10^{-11}\times\exp(80/T)$	IUPAC
MEK + Cl → MEKCO2 + HCl	$2.4\times10^{-12}\times\exp(80/T)$	IUPAC
MPRK + Cl → CO2C54O2 + HCl	9.6×10^{-11}	b
MPRK + Cl → MPRKAO2 + HCl	2.1×10^{-11}	b
DIEK + Cl → DIEKAO2 + HCl	2.4×10^{-11}	b
DIEK + Cl → DIEKBO2 + HCl	2.4×10^{-11}	b
MIPK + Cl → MIPKAO2 + HCl	3.5×10^{-11}	b
MIPK + Cl → MIPKBO2 + HCl	3.2×10^{-11}	b
HEX2ONE + Cl → HEX2ONAO2 + HCl	1.56×10^{-10}	b
HEX2ONE + Cl → HEX2ONBO2 + HCl	3.5×10^{-11}	b
HEX2ONE + Cl → HEX2ONCO2 + HCl	2.7×10^{-11}	b
HEX3ONE + Cl → HEX3ONAO2 + HCl	1.05×10^{-10}	b
HEX3ONE + Cl → HEX3ONBO2 + HCl	2.3×10^{-11}	b
HEX3ONE + Cl → HEX3ONCO2 + HCl	1.8×10^{-11}	b
HEX3ONE + Cl → HEX3ONDO2 + HCl	1.8×10^{-11}	b
MIBK + Cl → MIBKAO2 + HCl	3.1×10^{-10}	b
MIBK + Cl → MIBKBO2 + HCl	3.0×10^{-11}	b
MTBK + Cl → MTBKO2 + HCl	2.9×10^{-11}	b
CYHEXONE + Cl → CYHXONAO2 + HCl	1.3×10^{-10}	b
Alcohols + Cl		
CH3OH + Cl → HO2 + HCHO + HCl	$7.1\times10^{-11}\times\exp(-75/T)$	IUPAC
C2H5OH + Cl → CH3CHO + HO2 + HCl	$5.5\times10^{-11}\times\exp(155/T)$	IUPAC

C2H5OH + Cl → HOCH2CH2O2 + HCl	$4.8\times10^{-12}\times$ exp (155/T)	IUPAC
NPROPOL+ Cl → C2H5CHO + HO2 + HCl	$1.6\times10^{-11}\times$ exp (525/T)	IUPAC
NPROPOL + Cl → HO1C3O2 + HCl	$4.1\times10^{-12}\times$ exp (525/T)	IUPAC
NPROPOL + Cl → HYPROPO2 + HCl	$6.8\times10^{-12}\times$ exp (525/T)	IUPAC
IPROPOL + Cl → CH3COCH3 + HO2 + HCl	7.4×10^{-11}	IUPAC
IPROPOL + Cl → IPROPOLO2 + HCl	1.3×10^{-11}	IUPAC
NBUTOL+ Cl → C3H7CHO + HO2 + HCl	$1.25\times10^{-11}\times$ exp (550/T)	IUPAC
NBUTOL + Cl → NBUTOLAO2 + HCl	$1.12\times10^{-11}\times$ exp (550/T)	IUPAC
NBUTOL + Cl → NBUTOLBO2 + HCl	$1.12\times10^{-11}\times$ exp (550/T)	IUPAC
BUT2OL + Cl → BUT2OLO2 + HCl	5.37×10^{-11}	b
BUT2OL + Cl → MEK + HO2 + HCl	9.51×10^{-11}	b
IBUTOL + Cl → IBUTOLBO2 + HCl	$2.6\times10^{-11}\times$ exp (352/T)	b
IBUTOL + Cl → IBUTOLCO2 + HCl	$4.2\times10^{-12}\times$ exp (352/T)	b
IBUTOL + Cl → IPRCHO + HO2 + HCl	$1.6\times10^{-11}\times$ exp (352/T)	b
TBUTOL+ Cl → TBUTOLO2 + HCl	$2.4\times10^{-11}\times$ exp (-121/T)	b
TBUTOL+ Cl → TC4H9O + HCl	$3.1\times10^{-12}\times$ exp (-121/T)	b
PECOH + Cl → DIEK + HO2 + HCl	9.1×10^{-11}	b
PECOH + Cl → HO3C5O2 + HCl	1.5×10^{-11}	b
PECOH + Cl → PE2ENEBO2 + HCl	1.0×10^{-10}	b
IPEAOH+ Cl → BUT2CHO + HO2 + HCl	5.5×10^{-11}	b
IPEAOH + Cl → HM2C43O2 + HCl	4.9×10^{-11}	b
IPEAOH + Cl → M2BUOL2O2 + HCl	8.7×10^{-11}	b
ME3BUOL+Cl → C3ME3CHO+HO2 + HCl	6.45×10^{-11}	b
ME3BUOL + Cl → HM33C3O2 + HCl	1.02×10^{-10}	b
ME3BUOL + Cl → ME3BUOLO2 + HCl	5.78×10^{-11}	b
IPECOH + Cl → HO2M2C4O2 + HCl	6.58×10^{-12}	b
IPECOH + Cl → ME2BU2OLO2 + HCl	4.62×10^{-11}	b
IPECOH + Cl → PROL11MO2 + HCl	1.31×10^{-11}	b
IPEBOH + Cl → H2M3C4O2 + HCl	1.57×10^{-11}	b
IPEBOH + Cl → ME2BUOLO2 + HCl	9.82×10^{-11}	b
IPEBOH + Cl → MIPK + HO2 + HCl	9.82×10^{-11}	b
CYHEXOL+ Cl → CYHEXOLAO2 + HCl	2.2×10^{-10}	b
CYHEXOL + Cl → CYHEXONE+HO2+ HCl	7.9×10^{-11}	b
MIBKAOH+ Cl → MIBKAOHAO2+ HCl	3.4×10^{-11}	b
MIBKAOH+ Cl → MIBKAOHBO2+ HCl	1.3×10^{-11}	b
MIBKAOH + Cl → MIBKHO4O2 + HCl	1.8×10^{-12}	b
ETHGLY+ Cl → HOCH2CHO+HO2+ HCl	2.5×10^{-10}	b
PROPGLY+ Cl → ACETOL + HO2 + HCl	1.26×10^{-10}	b
PROPGLY+ Cl → CH3CHOHCHO + HO2 + HCl	7.94×10^{-11}	b
CRESOL + Cl → OXYL1O2 + HCl	6.20×10^{-11}	e

Organic acids + Cl		
CH3OOH + Cl → CH3O2 + HCl	3.54×10^{-11}	IUPAC
CH3OOH + Cl → HCHO + OH + HCl	2.36×10^{-11}	IUPAC
HCOOH + Cl → HO2 + HCl	1.9×10^{-13}	IUPAC
CH3CO2H + Cl → CH3O2 + HCl	2.65×10^{-14}	IUPAC
PROPACID + Cl → C2H5O2 + HCl	3.96×10^{-14}	b
Organic nitrates + Cl		
CH3NO3 + Cl → HCHO + NO2 + HCl	2.4×10^{-13}	IUPAC
C2H5NO3 + Cl → CH3CHO + NO2 + HCl	4.7×10^{-12}	IUPAC
NC3H7NO3 + Cl → C2H5CHO + NO2 + HCl	2.2×10^{-11}	IUPAC
IC3H7NO3 + Cl → CH3COCH3 + NO2 + HCl	3.8×10^{-12}	IUPAC
NC4H9NO3 + Cl → C3H7CHO + NO2 + HCl	8.5×10^{-11}	IUPAC
Aromatics + Cl		
TOLUENE + Cl → C6H5CH2O2 + HCl	5.9×10^{-11}	Shi and Bernhard, 1997
OXYL + Cl → OXYLO2 + HCl	1.5×10^{-10}	Shi and Bernhard, 1997
MXYL + Cl → MXYLO2 + HCl	1.7×10^{-10}	b
PXYL + Cl → PXYLO2 + HCl	2.6×10^{-10}	b
EBENZ + Cl → C6H5C2H4O2 + HCl	9.1×10^{-11}	b
PBENZ + Cl → PHC3O2 + HCl	7.5×10^{-11}	b
IPBENZ + Cl → PHIC3O2 + HCl	8.2×10^{-11}	b
TM123B + Cl → TM123BO2 + HCl	3.6×10^{-10}	b
TM124B + Cl → TM124BO2 + HCl	3.6×10^{-10}	b
TM135B + Cl → TMBO2 + HCl	3.1×10^{-10}	b
OETHTOL + Cl → ETOLO2 + HCl	1.1×10^{-10}	b
METHTOL + Cl → ETOLO2 + HCl	1.4×10^{-10}	b
PETHTOL + Cl → ETOLO2 + HCl	2.2×10^{-10}	b
Alkenes + Cl		
C2H4 + Cl → CH2CLCH2O2	1.0×10^{-10}	IUPAC
C3H6 + Cl → C3H5O2 + HCl	2.7×10^{-11}	Riedel et al. 2014
C3H6 + Cl → IPROCLO2	1.35×10^{-10}	Riedel et al. 2014
C3H6 + Cl → HYPROCLO2	1.08×10^{-10}	Riedel et al. 2014
OLEFIN + Cl → OLECLO2	5.86×10^{-10}	b, g
C5H8 + Cl → ISOCLO2	$1.28\times10^{-10}\times\exp(390/T)$	CB04
Alkyne + Cl		
C2H2 + Cl → CLCHO + CO + HO2	4.97×10^{-11}	h

[a] All species are variables existing in the MCM, except for 'OLEFIN' and some reaction products of Cl with C_3H_6, OLEFIN, C_5H_8 and ethyne.

[b] Reaction with Cl is assumed to be similar to that with OH, and the Cl rate constant is calculated by multiplying the OH rate constant by the average k_{Cl}/k_{OH} for compounds with available kinetic data (note that the C1 species was excluded from the k_{Cl}/k_{OH} calculation).

[c] The mechanism is taken from the SAPRC07 (http://www.engr.ucr.edu/~carter/SAPRC/saprc07.pdf).

[d] 45% of MACR is oxidized by Cl as a common aldehyde, whilst the remainder is treated as an alkene, being lumped into the 'OLEFIN'.

[e] The mechanism is taken from the SAPRC07 (http://www.engr.ucr.edu/~carter/SAPRC/saprc07.pdf). The reaction yields a new RO_2 radical, the degradation of which is approximated for simplicity to be the same as that of OXYL1O2.

[f] Reactions of Cl with C_3H_6, OLEFIN and C_5H_8 introduce new model species and further reactions (see *Xue et al.* 2015 for the further reactions).

[g] OLEFIN is defined in the present study as the sum of 1-butene, i-butene, trans-2-butene, cis-2-butene, 1-pentene, trans-2-pentene, cis-2-pentene, 1-hexene, 2-methyl-1-butene, 3-methyl-1-butene, 2-methyl-2-butene, trans-2-hexene, cis-2-hexene, 2,3-dimethyl-2-butene, styrene, MVK and MACR (55%).

[h] The mechanism is taken from the SAPRC07 (http://www.engr.ucr.edu/~carter/SAPRC/saprc07.pdf). CLCHO is a new species in the MCM, but is assumed to be less reactive and not considered for further reactions.

1.2. Physical processes

1.2.1. Photolysis frequencies

In the OBM-AOCP, photolysis frequencies (*J* values) are computed as a function of solar zenith angle (SZA), as defined by Saunders et al. (2003). To account for the potential impacts of cloud cover and particles, the model-calculated *J* values were further scaled in the present study with the measured J_{NO2} data, which were read in the model at a time interval of 10 minutes.

1.2.2. Dilution mixing with evolution of the planetary boundary layer

The dilution mixing was considered for all model species by introducing a dilution factor, which is defined as a function of the change in the height of planetary boundary layer (PBL). In the present study, the PBL height was assumed to vary linearly from 300 m at night to 1500 m at 14:00 local time in the afternoon. Sensitivity model runs with other maximum PBL heights (e.g., 1000 m and 2000 m) indicated that its impacts on the modeling results are negligible (i.e., <3% for modeled radical concentrations and primary source strengths of OH).

1.2.3. Dry Deposition

Dry deposition was considered for various inorganic gases and organic species including PANs, carbonyls, organic peroxides and acids in our model. The dry deposition velocities are taken from the literature of Zhang et al. (2003).

1.3. Observational Constraint

The model was constrained in real-time with a full suite of measurement data to simulate the in-situ atmospheric chemistry. In the present study, it was constrained by the observed diurnal data of CO, NO, NO_2, SO_2, O_3, H_2O_2, HONO, $ClNO_2$, PAN, CH_4, C_2-C_{10} NMHCs, C_1-C_8 carbonyls, aerosol surface area and radius, RH, temperature, pressure and J_{NO2}. The observational data were averaged or interpolated with a time resolution of 10 minutes as the model constraints. The model was made with 00:00 LT as the initial time and ran for a 24-hour period. Before each simulation, the model was pre-run for five days with constraints of the campaign-average data so as to reach a steady state for the unconstrained species (e.g., radicals). Finally, the model outputs were extracted and applied for further analyses.

2. Model-simulated RO_X levels

Figure S6 shows the model-predicted daytime concentrations of OH, HO_2 and RO_2 at TC during the two episodes. The maximum concentrations of OH, HO_2 and RO_2 were 6.4×10^6, 7.7×10^8 and 9.2×10^8 molecules cm^{-3} (equivalent as 0.27, 32 and 39 pptv) on 25 August, and were 7.0×10^6, 5.3×10^8 and 4.8×10^8 molecules cm^{-3} (0.30, 23 and 20 pptv) on 31 August. To put our simulated results in a global perspective, the RO_X radical levels at TC are well within the measured or modeled ranges in the polluted urban environments (Stone et al., 2012; and references therein). For instance, the peak concentrations of OH and HO_2 in Hong Kong are higher than those measured in Los Angeles U.S. (George et al., 1999), Birmingham U.K. (Emmerson et al., 2005) and Tokyo Japan (Kanaya et al., 2007), similar to those in New York U.S. (Ren et al., 2003) and Mexico City Mexico (Dusanter et al., 2009; Shirley et al., 2006), and lower than those in Nashville U.S. (Martinez et al., 2003) and Houston U.S. (Mao et al., 2010). In comparison with the limited results available in China, the RO_X levels at TC are comparable to those simulated in Beijing (Liu et al., 2012) and Mt. Tai (Kanaya et al., 2009).

It is noteworthy that our simulated concentrations of OH/HO_2 are much lower than the measured levels at a rural site (Back Garden) in the northern PRD (Hofzumahaus et al., 2009). The discrepancy may be due to the difference in the environments (e.g., high-NO_X condition at TC and low-NO_X condition at Back Garden) and/or the deficiency of current models to represent radical chemistry. Without direct observations of HO_X, it is impossible to address the potential 'discrepancy' between measured and modeled radical levels, which is usually

found in the low-NO_X environments. Here, the rationale of this study is to identify the major species and reaction pathways affecting the radical chemistry in the high-NO_X environment of Hong Kong and the PRD region, based on the 'known chemistry' and comprehensive measurements of related parameters. Obviously, direct measurements of HO_X radicals are quite needed to pin down this issue in the high-NO_X environment of Hong Kong and the PRD region.

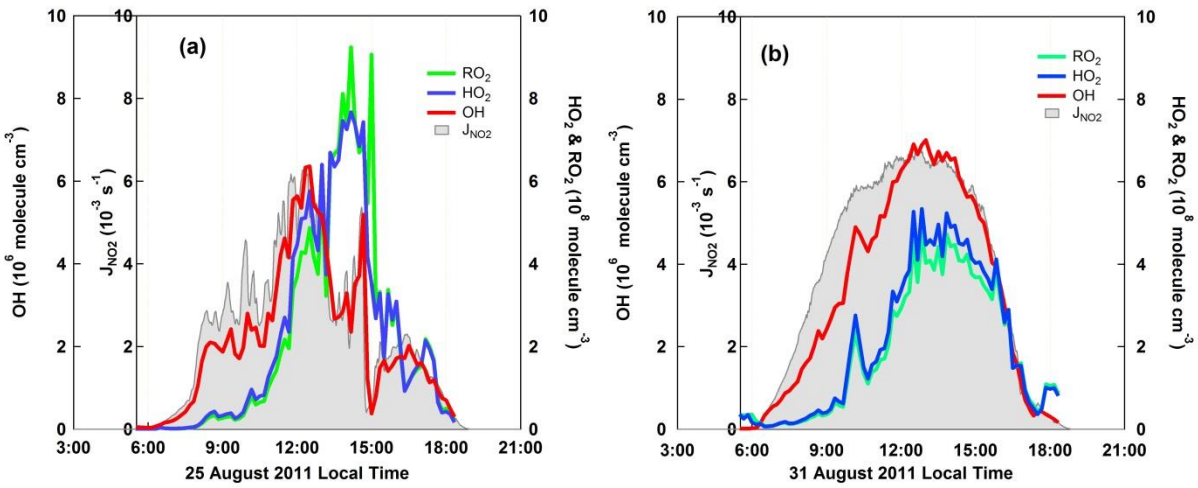

Figure S6. Model-simulated daytime concentrations of OH, HO_2 and RO_2 radicals at Tung Chung on (a) 25 August 2011 and (b) 31 August 2011.

References

Dusanter, S., Vimal, D., Stevens, P. S., Volkamer, R., Molina, L. T., Baker, A., Meinardi, S., Blake, D., Sheehy, P., Merten, A., Zhang, R., Zheng, J., Fortner, E. C., Junkermann, W., Dubey, M., Rahn, T., Eichinger, B., Lewandowski, P., Prueger, J., and Holder, H.: Measurements of OH and HO_2 concentrations during the MCMA-2006 field campaign - Part 2: Model comparison and radical budget, *Atmos Chem Phys*, 9, 6655-6675, 2009.

Emmerson, K. M., Carslaw, N., and Pilling, M. J.: Urban atmospheric chemistry during the PUMA campaign 2: Radical budgets for OH, HO_2 and RO_2, *J Atmos Chem*, 52, 165-183, 2005.

George, L. A., Hard, T. M., and O'Brien, R. J.: Measurement of free radicals OH and HO_2 in Los Angeles smog, *J Geophys Res-Atmos*, 104, 11643-11655, 1999.

Hofzumahaus, A., Rohrer, F., Lu, K. D., Bohn, B., Brauers, T., Chang, C. C., Fuchs, H.,

Holland, F., Kita, K., Kondo, Y., Li, X., Lou, S. R., Shao, M., Zeng, L. M., Wahner, A., and Zhang, Y. H.: Amplified Trace Gas Removal in the Troposphere, *Science*, 324, 1702-1704, 2009.

Jenkin, M. E., Saunders, S. M., Wagner, V., and Pilling, M. J.: Protocol for the development of the Master Chemical Mechanism, MCM v3 (Part B): tropospheric degradation of aromatic volatile organic compounds, *Atmos Chem Phys*, 3, 181-193, 2003.

Kanaya, Y., Cao, R. Q., Akimoto, H., Fukuda, M., Komazaki, Y., Yokouchi, Y., Koike, M., Tanimoto, H., Takegawa, N., and Kondo, Y.: Urban photochemistry in central Tokyo: 1. Observed and modeled OH and HO_2 radical concentrations during the winter and summer of 2004, *J Geophys Res-Atmos*, 112, 2007.

Kanaya, Y., Pochanart, P., Liu, Y., Li, J., Tanimoto, H., Kato, S., Suthawaree, J., Inomata, S., Taketani, F., Okuzawa, K., Kawamura, K., Akimoto, H., and Wang, Z. F.: Rates and regimes of photochemical ozone production over Central East China in June 2006: a box model analysis using comprehensive measurements of ozone precursors, *Atmos Chem Phys*, 9, 7711-7723, 2009.

Liu, Z., Wang, Y., Gu, D., Zhao, C., Huey, L. G., Stickel, R., Liao, J., Shao, M., Zhu, T., Zeng, L., Amoroso, A., Costabile, F., Chang, C. C., and Liu, S. C.: Summertime photochemistry during CAREBeijing-2007: ROx budgets and O_3 formation, *Atmos Chem Phys*, 12, 7737-7752, 2012.

Mao, J. Q., Ren, X. R., Chen, S. A., Brune, W. H., Chen, Z., Martinez, M., Harder, H., Lefer, B., Rappengluck, B., Flynn, J., and Leuchner, M.: Atmospheric oxidation capacity in the summer of Houston 2006: Comparison with summer measurements in other metropolitan studies, *Atmos Environ*, 44, 4107-4115, 2010.

Martinez, M., Harder, H., Kovacs, T. A., Simpas, J. B., Bassis, J., Lesher, R., Brune, W. H., Frost, G. J., Williams, E. J., Stroud, C. A., Jobson, B. T., Roberts, J. M., Hall, S. R., Shetter, R. E., Wert, B., Fried, A., Alicke, B., Stutz, J., Young, V. L., White, A. B., and Zamora, R. J.: OH and HO_2 concentrations, sources, and loss rates during the Southern Oxidants Study in Nashville, Tennessee, summer 1999, *J Geophys Res-Atmos*, 108, 2003.

Ren, X. R., Harder, H., Martinez, M., Lesher, R. L., Oliger, A., Simpas, J. B., Brune, W. H.,

Schwab, J. J., Demerjian, K. L., He, Y., Zhou, X. L., and Gao, H. G.: OH and HO_2 chemistry in the urban atmosphere of New York City, *Atmos Environ*, 37, 3639-3651, 2003.

Saunders, S. M., Jenkin, M. E., Derwent, R. G., and Pilling, M. J.: Protocol for the development of the Master Chemical Mechanism, MCM v3 (Part A): tropospheric degradation of non-aromatic volatile organic compounds, *Atmos Chem Phys*, 3, 161-180, 2003.

Shirley, T. R., Brune, W. H., Ren, X., Mao, J., Lesher, R., Cardenas, B., Volkamer, R., Molina, L. T., Molina, M. J., Lamb, B., Velasco, E., Jobson, T., and Alexander, M.: Atmospheric oxidation in the Mexico City Metropolitan Area (MCMA) during April 2003, *Atmos Chem Phys*, 6, 2753-2765, 2006.

Stone, D., Whalley, L. K., and Heard, D. E.: Tropospheric OH and HO_2 radicals: field measurements and model comparisons, *Chem Soc Rev*, 41, 6348-6404, 2012.

Wang, T., Tham, Y. J., Xue, L. K., Li, Q. Y., Zha, Q. Z., Wang, Z., Poon, C. N., Dube, W. P., Blake, D. R., Louie, P. K. K., Luk, C. W. Y., Tsui, W., Brown, S. S.: Observations of nitryl chloride and modeling its source and effect on ozone in the planetary boundary layer of southern China, J. Geophys. Res., 121, 5, 2016.

Xue, L. K., Wang, T., Guo, H., Blake, D. R., Tang, J., Zhang, X. C., Saunders, S. M., and Wang, W. X.: Sources and photochemistry of volatile organic compounds in the remote atmosphere of western China: results from the Mt. Waliguan Observatory, *Atmos Chem Phys*, 13, 8551-8567, 2013.

Xue, L. K., Wang, T., Gao, J., Ding, A. J., Zhou, X. H., Blake, D. R., Wang, X. F., Saunders, S. M., Fan, S. J., Zuo, H. C., Zhang, Q. Z., and Wang, W. X.: Ground-level ozone in four Chinese cities: precursors, regional transport and heterogeneous processes, *Atmos Chem Phys*, 14, 13175-13188, 2014a.

Xue, L. K., Wang, T., Louie, P. K. K., Luk, C. W. Y., Blake, D. R., and Xu, Z.: Increasing External Effects Negate Local Efforts to Control Ozone Air Pollution: A Case Study of Hong Kong and Implications for Other Chinese Cities, *Environ Sci Technol*, 48, 10769-10775, 2014b.

Xue, L. K., Wang, T., Wang, X. F., Blake, D. R., Gao, J., Nie, W., Gao, R., Gao, X. M., Xu, Z.,

Ding, A. J., Huang, Y., Lee, S. C., Chen, Y. Z., Wang, S. L., Chai, F. H., Zhang, Q. Z., and Wang, W. X.: On the use of an explicit chemical mechanism to dissect peroxy acetyl nitrate formation, *Environ Pollut*, 195, 39-47, 2014c.

Xue, L. K., Saunders, S. M., Wang, T., Gao, R., Wang, X. F., Zhang, Q. Z., and Wang, W. X.: Development of a chlorine chemistry module for the Master Chemical Mechanism, *Geosci Model Dev*, 8, 3151-3162, 2015.

Zhang, L., Brook, J. R., and Vet, R.: A revised parameterization for gaseous dry deposition in air-quality models, *Atmos. Chem. Phys.*, 3, 2067-2082, 2003.